Consensus based odour source localisation by multi-agent systems

Abhinav Sinha, Rishemjit Kaur, Ritesh Kumar, Amol P Bhondekar

Consensus based odour source localisation by multi-agent systems

Abhinav Sinha, Rishemjit Kaur, Ritesh Kumar and Amol P. Bhondekar

***Abstract*—This paper presents an investigation of the task of localising unknown source of an odour by heterogeneous multi-agent systems. A hierarchical cooperative control strategy has been proposed as a potential candidate to solve the problem. The agents are driven into consensus as soon as the information about the location of source is acquired. The controller has been designed in a hierarchical manner of group decision making, agent path planning, and robust control. In group decision making, a Particle Swarm Algorithm has been used along with the information of the movement of odour molecules to predict the odour source location. Next, a trajectory has been mapped using this predicted location of source, and the information is passed to the control layer. A variable structure control has been used in the control layer due to its inherent robustness and disturbance rejection capabilities. Cases of movement of agents towards the source under consensus, and parallel formation have been discussed. The efficacy of the proposed scheme has been confirmed by simulations.**

I. Introduction

Research in robot olfaction has received wide attention to address many challenges, some of which include detection of forest fire, hazardous gases in mines, tunnels and industrial setup, search and rescue of victims [1]–[3]. Recently, odour source localisation via autonomous agents on other planets such as Mars has also been carried out [4], [5]. Numerous simple and complex algorithms for olfaction problems have imitated behaviour of biological entities such as mate seeking by moths, foraging by lobsters, prey tracking by mosquitoes and blue crabs, etc. However, techniques like probabilistic inference [6], [7], robust control [8], swarm intelligence [9], biased random walk [10], optimisation and meta-heuristics prove better in localisation than aforementioned techniques.

Works on odour source localisation in early 90s were mostly targeted via chemical gradient based techniques in a diffusion dominated environment [11]–[14]. In practice, this assumption leads to sub-optimal performance for above-ground agents due to the geometry and dimensions of the agents. This assumption, however, yields satisfactory performance in underground search [15]–[17]. Difficulties associated with diffusion dominated odour dispersal model led to the development of reactive plume tracking approaches, the performance of which was further improved by combining vision with sensing [18]–[20]. The efficiency of techniques depending heavily on sensing, such as chemotaxis [21], anemotaxis [6], [22], infotaxis [7], fluxotaxis [23] and their close variants are limited by the quality of sensors and the manner in which they are used. Bio-inspired agent manoeuvreing such as Braitenberg style [24], E. coli algorithm [10], Zigzag dung beetle approach [25], silkworm moth style [15], [26], [27] are slow in localisation. Many of these localising techniques deliver unsatisfactory tracking performance in a turbulence dominated environment.

With advantages of multi-agent systems (MAS) such as spatial diversity, distributed sensing and actuation, redundancy, scalability, high reliability and increased probability of success, odour source localisation can be effectively solved. This dynamical optimisation problem is characterised by three stages– instantaneous plume sensing (plume finding), manoeuvreing of the agents (plume traversal) and cooperative control of the agents. In spite of a growing attention from researchers in the last decade [28]–[31], only a few works have addressed odour source localisation using MAS. A distributed cooperative algorithm based on swarm intelligence was put forth by Hayes *et al.* [32] and experimental results proved multiple robots perform more efficiently than a single autonomous robot. Marques *et al.* proposed Particle Swarm optimisation (PSO) algorithm [33] to localise odour source. Studies in [34] reported modified PSO technique based on electrical charge theory by using neutral and charged robots to find the odour source without getting trapped into a local maximum concentration. Distributed control based on simplified PSO was proposed by Lu *et al.* in [35], which is a type of proportional-only controller and the operating region is confined between global and local best. This requires complicated obstacle avoidance algorithms and more energy consumption. Odour propagation is non-trivial, i.e., odour arrives in packets, leading to wide fluctuations in measured concentrations. Plumes also tend to be dynamic and turbulent. In order to effectively solve odour source localisation problem, the information of wind needs to be taken into consideration. As odour molecules travel downwind, direction of the wind provides an effective information on relative position of the source. Using both concentration and wind information, Lu *et al.* have designed a particle filter based cooperative control scheme [36] to coordinate multiple robots towards odour source. However, the dynamical model used in [35], [36] are oversimplified to integrator dynamics and the effects of unknown perturbations have not been considered. To address the effect of perturbations, robust control protocols have been designed in [8], [37], but the dynamics of the MAS is homogeneous, i.e, agents are identical. In practice it is very difficult to obtain truly homogeneous agents. Even

A. Sinha is with School of Mechatronics & Robotics, Indian Institute of Engineering Science and Technology; and Central Scientific Instruments Organisation (CSIR- CSIO), India.
email: sinha.abhinav.pg2016@mechatronics.iiests.ac.in
R. Kaur, R. Kumar & A. P. Bhondekar are with CSIR- CSIO.
emails: rishemjit.kaur@csio.res.in, riteshkr@csio.res.in, amolbhondekar@csio.res.in

truly homogeneous agents exhibit a tendency to drift towards heterogeneity over time and continued operation.

In spite of rapid developments in sensor technology, availability of faster localisation algorithms are still a challenge. Motivated by these studies and in order to effectively address the odour source localisation problem, we have proposed a three-layered hierarchical cooperative control scheme which uses concentration information from swarm, as well as wind information from a measurement model [38] describing movement of filaments to locate the odour source. Information about the source via instantaneous sensing and swarm intelligence is obtained in the first layer. Second layer is designed to manoeuvre the agents via traditional surging, casting and searching methods. Third layer is the cooperative control layer and the cooperative controller is based on the paradigms of variable structure control (*aka* sliding mode control), which is known for its inherent robustness and properties to reject disturbances that lie in the range space of input. In the third layer, the information obtained in the first layer is passed as a reference to the tracking controller. A block diagram representation of the proposed scheme has been shown in figure 1. The idea of using a finite time controller is not

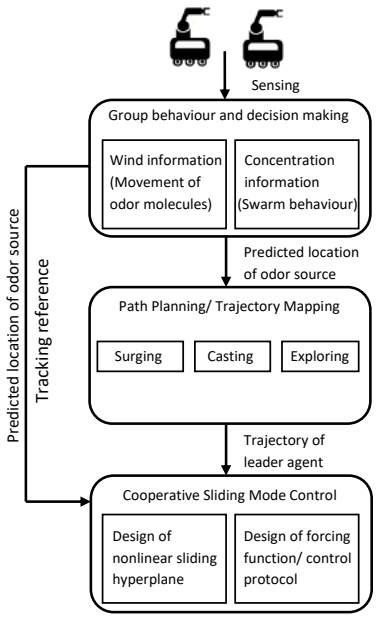

Fig. 1: Proposed hierarchical cooperative control scheme for odor source localization

new, however we have adopted a different perspective in this study. To the best of authors' knowledge, sliding mode control technique with novel manifold and reaching law has been used for the first time in odour source localisation. The sole idea to use such a control is to guarantee faster convergence, complete disturbance rejection and steady precision. Moreover, studies in this work incorporate a large class of systems that may contain unknown inherent nonlinearity and heterogeneity. We summarise our contributions via following points.

- Individual autonomous agents may have some inherent nonlinear dynamics. This work generalises the problem by taking into account nonlinear dynamics of MAS. When the uncertain function is zero, the dynamics simply reduces to that of an integrator system.
- Individual autonomous agents might have different dynamics for a practical application. Hence, the consideration of heterogeneous agent dynamics is more close to real situations.
- The finite time robust controller is based on sliding modes with nonlinear sliding hyperplane and novel inverse sine hyperbolic based reaching law. Consequently, the control signal is smooth and reachability to the manifold is fast.
- The synthesised control ensures stability even in the presence of disturbances that are bounded and matched.

After introduction to the study in section 1, remainder of this work in organised as follows. Section 2 provides insights into preliminaries of spectral graph theory and sliding mode control. Section 3 presents dynamics of MAS and mathematical problem formulation, followed by hierarchical distributed cooperative control scheme in section 4. Results and discussions have been carried out in section 5, followed by concluding remarks in section 6.

II. Preliminaries

A. Spectral Graph Theory for Multi-Agent Systems

A directed graph, also known as digraph is represented throughout in this paper by $\mathcal{G} = (\mathcal{V}, \mathcal{E}, \mathcal{A})$. $\mathcal{V}$ is the nonempty set in which finite number of vertices or nodes are contained such that $\mathcal{V} = \{1, 2, ..., N\}$. $\mathcal{E}$ denotes directed edge and is represented as $\mathcal{E} = \{(i, j) \; \forall \; i, j \in \mathcal{V} \; \& \; i \neq j\}$. $\mathcal{A}$ is the weighted adjacency matrix such that $\mathcal{A} = a(i, j) \in \mathbb{R}^{\mathrm{N}\times\mathrm{N}}$. The possibility of existence of an edge (i, j) occurs iff the vertex i receives the information supplied by the vertex j, i.e., $(i, j) \in \mathcal{E}$. Hence, i and j are termed neighbours. The set $\mathcal{N}_i$ contains labels of vertices that are neighbours of the vertex i. For the adjacency matrix $\mathcal{A}$, $a(i, j) \in \mathbb{R}_0^+$. If $(i, j) \in \mathcal{E} \Rightarrow a(i, j) > 0$. If $(i, j) \notin \mathcal{E}$ or $i = j \Rightarrow a(i, j) = 0$. The Laplacian matrix $\mathcal{L}$ [39] is central to the consensus problem and is given by $\mathcal{L} = \mathcal{D} - \mathcal{A}$ where degree matrix, $\mathcal{D}$ is a diagonal matrix, i.e, $\mathcal{D}$ = diag$(d_1, d_2, ..., d_n)$ whose entries are $d_i = \sum_{j=1}^{n} a(i, j)$. A directed path from vertex j to vertex i defines a sequence comprising of edges $(i, i_1), (i_1, i_2), ..., (i_l, j)$ with distinct vertices $i_k \in \mathcal{V}$, $k = 1, 2, 3, ..., l$. Incidence matrix $\mathcal{B}$ is also a diagonal matrix with entries 1 or 0. The entry is 1 if there exists an edge between leader agent and any other agent, otherwise it is 0. Furthermore, it can be inferred that the path between two distinct vertices is not uniquely determined. However, if a distinct node in $\mathcal{V}$ contains directed path to every other distinct node in $\mathcal{V}$, then the directed graph $\mathcal{G}$ is said to have a spanning tree. Consequently,the matrix $\mathcal{L} + \mathcal{B}$ has full rank [39]. Physically, each agent has been modelled by a vertex or node and the line of communication between any two agents has been modelled as a directed edge.

B. Sliding Mode Control

Sliding Mode Control (SMC) [40] is known for its inherent robustness. The switching nature of the control is used

to nullify bounded disturbances and matched uncertainties. Switching happens about a hypergeometric manifold in state space known as sliding manifold, surface, or hyperplane. The control drives the system monotonically towards the sliding surface, i.e, trajectories emanate and move towards the hyperplane (reaching phase). System trajectories, after reaching the hyperplane, get constrained there for all future time (sliding phase), thereby ensuring the system dynamics remains independent of bounded disturbances and matched uncertainties.

In order to push state trajectories onto the surface $s(x)$, a proper discontinuous control effort $u_{\text{SM}}(t,x)$ needs to be synthesised satisfying the following inequality.

$$s^T(x)\dot{s}(x) \leq -\eta\|s(x)\|, \tag{1}$$

with η being positive and is referred as the reachability constant.

$$\because \quad \dot{s}(x) = \frac{\partial s}{\partial x}\dot{x} = \frac{\partial s}{\partial x}f(t,x,u_{\text{SM}}) \tag{2}$$

$$\therefore \quad s^T(x)\frac{\partial s}{\partial x}f(t,x,u_{\text{SM}}) \leq -\eta\|s(x)\|. \tag{3}$$

The motion of state trajectories confined on the manifold is known as *sliding*. Sliding mode exists if the state velocity vectors are directed towards the manifold in its neighbourhood. Under such consideration, the manifold is called attractive, i.e., trajectories starting on it remain there for all future time and trajectories starting outside it tend to it in an asymptotic manner. Hence, in sliding motion,

$$\dot{s}(x) = \frac{\partial s}{\partial x}f(t,x,u_{\text{SM}}) = 0. \tag{4}$$

$u_{\text{SM}} = u_{eq}$ is a solution, generally referred as equivalent control is not the actual control applied to the system but can be thought of as a control that must be applied on an average to maintain sliding motion and is mainly used for analysis of sliding motion.

III. Dynamics of MAS & Problem Formulation

Consider first order heterogeneous MAS with a virtual leader and finite number of followers interacting among themselves and their environment in a well defined directed topology. Under such interconnection, only local information about the predicted location of source of the odour through instantaneous plume sensing is available via communication among agents. The governing dynamics of first order heterogeneous MAS that comprise of N agents can be written mathematically as

$$\dot{x}_i(t) = f_i(x_i(t)) + u_{\text{SM}_i}(t) + \varsigma_i; \quad i \in [1,N] \in \mathbb{N}, \tag{5}$$

where $f_i(\cdot)$ denotes the uncertain dynamics of each agent. x_i and u_{SM_i} are the state of i^{th} agent and the associated control respectively. ς_i represents bounded exogenous disturbances that enter the system from input channel, i.e., $\|\varsigma_i\| \leq \varsigma_{max} < \infty$.

Assumption III.1. *$f_i(\cdot) : \mathbb{R}^+ \times X \to \mathbb{R}^m$ is locally Lipschitz over some domain $\mathbb{D}_{\mathbb{L}}$ with Lipschitz constant $\bar{L}$. For our case, we shall take this domain $\mathbb{D}_{\mathbb{L}}$ to be fairly large. $X \subset \mathbb{R}^m$ is a domain in which origin is contained.*

Since the function $f_i(\cdot)$ is uncertain, a nominal system model can be extracted from the known part of the uncertain function $f_i(\cdot)$, and the unknown part can be treated by worst case bounds. The dynamics of each agent is affected by the interconnection among agents as well as the presence of inherent non-linearity in each agent. Note that when $f_i(\cdot) = 0$, the dynamics reduce to those of integrator systems.

Remark 1. For the sake of simplicity, we shall carry out the discussion in $\mathbb{R}^1$. However, the same can be extended to higher dimensions by the use of Kronecker products.

The problem of odour source localisation can be viewed as a cooperative control problem in which control laws u_{SM_i} need to be designed such that the conditions $\lim_{t\to\infty}\|x_i - x_j\| = 0$ and $\lim_{t\to\infty}\|x_i - x_s\| \leq \theta$ are satisfied. Here x_s represents the probable location of odour source & θ is an accuracy adjustment parameter in declaration of the true location of the source.

IV. Hierarchical Distributed Cooperative Control Scheme

In order to force the agents in consensus to locate the source of odour, we have come up with the following hierarchical scheme.

A. Group Decision Making

This layer utilises both concentration and wind information to predict the location of odour source. Then, the final probable position of the source can be described as

$$\phi(t_h) = k_1 p_i(t_h) + (1-k_1)q_i(t_h). \tag{6}$$

With the knowledge of PSO, $p_i(t_h)$ in (6) can be described as the oscillation centre. Information of the wind is captured in $q_i(t_h)$. $k_1 \in (0,1)$ denotes additional weighting coefficient.

Remark 2. Since the sensors equipped with the agents can only receive data at discrete instants, the arguments in (6) represent data captured at $t = t_h$ instants ($h = 1, 2, ...$).

It should be noted that ϕ is the tracking reference that is fed to the tracking controller. Now, we present detailed description of obtaining $p_i(t_h)$ and $q_i(t_h)$.

Commonly used simple PSO algorithm can be described in following form.

$$v_i(t_{h+1}) = \omega v_i(t_h) + u_{\text{PSO}}(t_h), \tag{7}$$

$$x_i(t_{h+1}) = x_i(t_h) + v_i(t_{h+1}). \tag{8}$$

Here ω is the inertia factor, $v_i(t_h)$ and $x_i(t_h)$ represent the respective velocity and position of i^{th} agent. This commonly used form of PSO can also be used as a proportional-only type controller, however for the disadvantages highlighted earlier, we do not regard PSO as our final controller. PSO control law u_{PSO} can be described as

$$u_{\text{PSO}} = \alpha_1(x_l(t_h) - x_i(t_h)) + \alpha_2(x_g(t_h) - x_i(t_h)). \tag{9}$$

In (9), $x_l(t_h)$ denotes the previous best position and $x_g(t_h)$ denotes the global best position of neighbours of i^{th} agent at time $t = t_h$, and α_1 & α_2 are acceleration coefficients. Since, every agent in MAS can get some information about the magnitude of concentration via local communication, position of the agent with a global best can be easily known. By the idea of PSO, we can compute the oscillation centre $p_i(t_h)$ as

$$p_i(t_h) = \frac{\alpha_1 x_l(t_h) + \alpha_2 x_g(t_h)}{\alpha_1 + \alpha_2}, \tag{10}$$

where

$$x_l(t_h) = \arg \max_{0<t<t_{h-1}} \{g(x_l(t_{h-1})), g(x_i(t_h))\}, \tag{11}$$

$$x_g(t_h) = \arg \max_{0<t<t_{h-1}} \{g(x_g(t_{h-1})), \max_{j \in N} a_{ij}\ g(x_j(t_h))\}. \tag{12}$$

Thus, from (9), (10)

$$u_{\text{PSO}}(t_h) = (\alpha_1 + \alpha_2)\{p_i(t_h) - x_i(t_h)\}, \tag{13}$$

which is clearly a proportional-only controller with proportional gain $\alpha_1 + \alpha_2$, as highlighted earlier.

In order to compute $q_i(t_h)$, movement process of a single filament that consists several odour molecules has been modelled based on study in [38]. If $x_f(t)$ denotes position of the filament at time t, $\bar{v}_a(t)$ represent mean airflow velocity and $n(t)$ be some random process, then the model can be described as

$$\dot{x}_f(t) = \bar{v}_a(t) + n(t). \tag{14}$$

Without loss of generality, we shall regard the start time of our experiment as $t = 0$. From (14), we have

$$x_f(t) = \int_0^t \bar{v}_a(\tau)d\tau + \int_0^t n(\tau)d\tau + x_s(0). \tag{15}$$

$x_s(0)$ denotes the real position of the odour source at $t = 0$.

Assumption IV.1. *We assume the presence of a single, stationary odour source. Thus, $x_s(t) = x_s(0)$.*

Implications from remark 2 require (15) to be implemented at $t = t_h$ instants. Hence,

$$x_f(t_h) = \sum_{m=0}^{t} \bar{v}_a(\tau_m)\Delta t + \sum_{m=0}^{t} n(\tau_m)\Delta t + x_s(t_h), \tag{16}$$

$$x_f(t_h) = x_s(t_h) + \bar{v}_a^\star(t_h) + w^\star(t_h). \tag{17}$$

In (17), $\sum_{m=0}^{t} \bar{v}_a(\tau_m)\Delta t = \bar{v}_a^\star(t_h)$ and $\sum_{m=0}^{t} n(\tau_m)\Delta t = w^\star(t_h)$.

Remark 3. In (17), the accumulated average of $\bar{v}_a^\star(t_h)$ and $w^\star(t_h)$ can also be considered for all possible filament releasing time.

From (17),

$$x_f(t_h) - \bar{v}_a^\star(t_h) = x_s(t_h) + w^\star(t_h). \tag{18}$$

The above relationship, (18) can be viewed as the information about $x_s(t_h)$ with some noise $w^\star(t_h)$. Hence,

$$q_i(t_h) = x_s(t_h) + w^\star(t_h). \tag{19}$$

Therefore, ϕ in (6) can now be constructed from (10) & (19).

B. Path Planning

The detection of information of interest based on instantaneous sensing of plume depends on the threshold value of sensors, and the next state is decided according to this threshold. Hence, the blueprints of trajectory planning can be described in terms of following behaviour.

- Surging: If the i^{th} agent receives data well above threshold, we say that some clues about the location of the source have been detected. If the predicted position of the source at $t = t_h$ as seen by i^{th} agent be given as $x_{s_i}(t_h)$, then the next state of the agent is given mathematically as
$$x_i(t_{h+1}) = x_{s_i}(t_h) \tag{20}$$
- Casting: If the i^{th} agent fails to detect information at any particular instant, then the next state is obtained using the following relation.
$$x_i(t_{h+1}) = \frac{\|x_i(t_h) - x_{s_i}(t_h)\|}{2} + x_{s_i}(t_h) \tag{21}$$
- Search and exploration: If all the agents fail to detect odour clues for a time segment $[t_h, t_{h+l}] > \delta_0$ for some $l \in \mathbb{N}$ and $\delta_0 \in \mathbb{R}^+$ being the time interval for which no clues are detected or some constraint on wait time placed at the start of the experiment, then the next state is updated as
$$x_i(t_{h+1}) = x_{s_i}(t_h) + \digamma_\sigma^\psi \tag{22}$$
In (22), $\digamma_\sigma^\phi$ is some random parameter with σ as its standard deviation and ψ as its mean.

C. Distributed Control

In the control layer, we design a robust and powerful controller on the paradigms of sliding mode. It is worthy to mention that based on instantaneous sensing and swarm information, at different times, each agent can take up the role of a virtual leader whose opinion needs to be kept by other agents. The trajectory is planned by the leader agent based on surging, casting and searching behaviour. ϕ from (6) has been provided to the controller as the reference to be tracked. The tracking error is formulated as

$$e_i(t) = x_i(t) - \phi(t_h)\ ; \quad t \in [t_h, t_{h+1}[. \tag{23}$$

In terms of graph theory, we can reformulate the error variable as

$$\epsilon_i(t) = (\mathcal{L} + \mathcal{B})e_i(t) = (\mathcal{L} + \mathcal{B})(x_i(t) - \phi(t_h)). \tag{24}$$

From this point onward, we shall denote $\mathcal{L} + \mathcal{B}$ as $\mathcal{H}$. Next, we propose the nonlinear sliding manifold

$$s_i(t) = \lambda_1 \tanh(\lambda_2 \epsilon_i(t)), \tag{25}$$

which offers faster reachability to the surface. $\lambda_1 \in \mathbb{R}^+$ represents the speed of convergence to the surface, and $\lambda_2 \in \mathbb{R}^+$ denotes the slope of the nonlinear sliding manifold. These are coefficient weighting parameters that affect the system performance. In linear sliding manifolds, the magnitude of

error is directly proportional to the magnitude of control effort needed to maintain sliding motion. In order to prevent violations of actuator constraints, the control effort is hard upper and lower bounded by some finite value, thereby making only a portion of the manifold attractive (termed as sliding regime). There is no guarantee of desired performance or stability outside the sliding regime. Moreover, if the reference state is too far from the current system state and the actuator saturates, the controller is unable to cope up, resulting in instability. Hence, it is beneficial to design nonlinear sliding manifolds that can hold the system states regardless of their location in the state space.

The forcing function has been proposed as

$$\dot{s}_i(t) = -\mu \sinh^{-1}(m + w|s_i(t)|)sign(s_i(t)). \tag{26}$$

In (26), m is a small offset such that the argument of $\sinh^{-1}(\cdot)$ function remains non zero and w is the gain of the controller. The parameter μ facilitates additional gain tuning. In general, $m << w$. This novel reaching law contains a nonlinear gain and provides faster convergence towards the manifold. Moreover, this reaching law is smooth and chattering free, which is highly desirable in mechatronic systems to ensure safe operation.

Theorem IV.1. *Given the dynamics of MAS (5) connected in a directed topology, error candidates (23, 24) and the sliding manifold (25), the stabilising control law that ensures accurate reference tracking under consensus can be described as*

$$u_{\mathrm{SM}_i}(t) = -\big\{(\Lambda\mathcal{H})^{-1}\mu \sinh^{-1}(m + w|s_i(t)|)sign(s_i(t))\Gamma^{-1} + (f(x_i(t)) - \dot{\phi}(t_h))\big\} \tag{27}$$

where $\Lambda = \lambda_1\lambda_2$, $\Gamma = 1 - \tanh^2(\lambda_2\epsilon_i(t))$, $w > \sup_{t\geq 0}\{\|\varsigma_i\|\}$ & $\mu > \sup\{\|\Lambda\mathcal{H}\varsigma_i\Gamma\|\}$.

Remark 4. As mentioned earlier, $\lambda_1, \lambda_2 \in \mathbb{R}^+$. This ensures $\Lambda \neq 0$ and hence its non singularity. The argument of $\tanh(\cdot)$ is always finite and satisfies $\lambda_2\epsilon_i(t) \neq \pi\iota(\kappa + 1/2)$ for $\kappa \in \mathbb{Z}$, thus Γ is also invertible. Moreover the non singularity of $\mathcal{H}$ can be established directly if the digraph contains a spanning tree with leader agent as a root.

Proof. From (24) and (25), we can write

$$\begin{aligned}
\dot{s}_i(t) &= \lambda_1\{\lambda_2\dot{\epsilon}_i(t)(1 - \tanh^2(\lambda_2\epsilon_i(t)))\} && (28)\\
&= \lambda_1\lambda_2\dot{\epsilon}_i(t) - \lambda_1\lambda_2\dot{\epsilon}_i(t)\tanh^2(\lambda_2\epsilon_i(t)) && (29)\\
&= \lambda_1\lambda_2\dot{\epsilon}_i(t)\{1 - \tanh^2(\lambda_2\epsilon_i(t))\} && (30)\\
&= \Lambda\mathcal{H}(\dot{x}_i(t) - \dot{\phi}(t_h))\Gamma && (31)
\end{aligned}$$

with Λ & Γ as defined in Theorem IV.1. From (5), (31) can be further simplified as

$$\dot{s}_i(t) = \Lambda\mathcal{H}(f(x_i(t)) + u_{\mathrm{SM}_i}(t) + \varsigma_i - \dot{\phi}(t_h))\Gamma. \tag{32}$$

Using (26), the control that brings the state trajectories on to the sliding manifold can now be written as

$$u_{\mathrm{SM}_i}(t) = -\big\{(\Lambda\mathcal{H})^{-1}\mu \sinh^{-1}(m + w|s_i(t)|)sign(s_i(t))\Gamma^{-1} + (f(x_i(t)) - \dot{\phi}(t_h))\big\},$$

which is same as (27), thereby completing the proof. □

Remark 5. The control (27) can be practically implemented as it does not contain the uncertainty term.

It is crucial to analyse the necessary and sufficient conditions for the existence of sliding mode when control protocol (27) is used. We regard the system to be in sliding mode if for any time $t_1 \in [0, \infty[$, system trajectories are brought upon the manifold $s_i(t) = 0$ and are constrained there for all time thereafter, i.e., for $t \geq t_1$, sliding motion occurs.

Theorem IV.2. *Consider the system described by (5), error candidates (23, 24), sliding manifold (25) and the control protocol (27). Sliding mode is said to exist in vicinity of sliding manifold, if the manifold is attractive, i.e., trajectories emanating outside it continuously decrease towards it. Stating alternatively, reachability to the surface is ensured for some reachability constant $\eta > 0$. Moreover, stability can be guaranteed in the sense of Lyapunov if gain μ is designed as $\mu > \sup\{\|\Lambda\mathcal{H}\varsigma_i\Gamma\|\}$.*

Proof. Let us take into account, a Lyapunov function candidate

$$V_i = 0.5s_i^2. \tag{33}$$

Taking derivative of (33) along system trajectories yield

$$\begin{aligned}
\dot{V}_i &= s_i\dot{s}_i && (34)\\
&= s_i\big\{\Lambda\mathcal{H}(f(x_i(t)) + u_{\mathrm{SM}_i}(t) + \varsigma_i - \dot{\phi}(t_h))\Gamma\big\}. && (35)
\end{aligned}$$

Substituting the control protocol (27) in (35), we have

$$\begin{aligned}
\dot{V}_i &= s_i\big(-\mu \sinh^{-1}(m + w|s_i|)sign(s_i) + \Lambda\mathcal{H}\varsigma_i\Gamma\big)\\
&= -\mu \sinh^{-1}(m + w|s_i|)\|s_i\| + \Lambda\mathcal{H}\varsigma_i\Gamma\|s_i\|\\
&= \big\{-\mu \sinh^{-1}(m + w|s_i|) + \Lambda\mathcal{H}\varsigma_i\Gamma\big\}\|s_i\|\\
&= -\eta\|s_i\|, && (36)
\end{aligned}$$

where $\eta = \mu \sinh^{-1}(m + w|s_i|) - \Lambda\mathcal{H}\varsigma_i\Gamma > 0$ is called reachability constant. For $\mu > \sup\{\|\Lambda\mathcal{H}\varsigma_i\Gamma\|\}$, we have

$$\dot{V}_i < 0. \tag{37}$$

Thus, the derivative of Lyapunov function candidate is negative definite confirming stability in the sense of Lyapunov.

Since, $\mu > 0$, $\|s_i\| > 0$ and $\sinh^{-1}(\cdot) > 0$ due to the nature of its arguments. Therefore, (36) and (26) together provide implications that $\forall s_i(0)$, $s_i\dot{s}_i < 0$ and the surface is globally attractive. This completes the proof. □

V. Results and Discussions

Figure 2 depicts the interaction topology of the agents [8] as a digraph. Note that although the developed theory and hierarchical scheme can be extended to a switching topology as well, we shall simplify the case by taking a fixed topology.

Assumption V.1. *Agent 1 appears as the virtual leader to all other agents. Therefore, the topology is fixed and directed.*

The associated graph matrices have been described below.

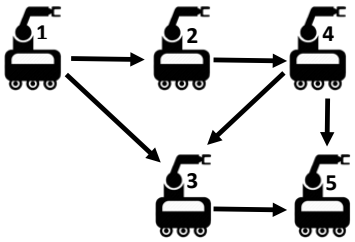

Fig. 2: Topology in which agents are connected

$$\mathcal{A} = \begin{bmatrix} 0&0&1&0 \\ 0&0&0&0 \\ 0&1&0&0 \\ 0&0&1&0 \end{bmatrix}, \quad \mathcal{B} = \begin{bmatrix} 1&0&0&0 \\ 0&1&0&0 \\ 0&0&0&0 \\ 0&0&0&0 \end{bmatrix}, \quad \mathcal{D} = \begin{bmatrix} 1&0&0&0 \\ 0&0&0&0 \\ 0&0&1&0 \\ 0&0&0&1 \end{bmatrix},$$

$$\mathcal{L} = \mathcal{D} - \mathcal{A} = \begin{bmatrix} 1&0&-1&0 \\ 0&0&0&0 \\ 0&-1&1&0 \\ 0&0&-1&1 \end{bmatrix}, \mathcal{L} + \mathcal{B} = \begin{bmatrix} 2&0&-1&0 \\ 0&1&0&0 \\ 0&-1&1&0 \\ 0&0&-1&1 \end{bmatrix} \tag{38}$$

Dynamics of the agents considered are described below.

$$\dot{x}_1 = 0.1\sqrt[3]{\sin(x_1)} + \cos(2\pi t) + u_{\mathrm{SM}_1}(t) + \varsigma_1, \tag{39}$$
$$\dot{x}_2 = 0.1\sin(x_2) - \cos(e^{-x_2 t}) + u_{\mathrm{SM}_2}(t) + \varsigma_2, \tag{40}$$
$$\dot{x}_3 = 0.1\sqrt[3]{\sin(x_3)} + \cos^2(2\pi t) + u_{\mathrm{SM}_3}(t) + \varsigma_3, \tag{41}$$
$$\dot{x}_4 = 0.1\sin(x_4) + \cos(x_4) + u_{\mathrm{SM}_4}(t) + \varsigma_4, \tag{42}$$
$$\dot{x}_5 = 0.1\cos(x_5) - \cos(2\pi t) - e^{-t} + u_{\mathrm{SM}_5}(t) + \varsigma_5. \tag{43}$$

Odour molecules tend to disperse heavily in the environment characterised by diffusion. In making assumption of a diffusion dominated environment, several factors are ignored. A more realistic picture must include effects of wind, turbulence diffusion and thermal effects. However, effects of turbulence are difficult to be described mathematically. In addition to the effects of wind, the characteristics of environment can also be described by advection phenomenon. Hence, we have considered a diffusion-advection plume model in our discussed source localisation problem. Before we begin to use this model, following assumptions need to be stated.

Assumption V.2. *We assume uniform airflow velocity for all time and throughout the domain in which the task of source localisation is being performed.*

Assumption V.3. *The turbulence diffusion coefficient K needs to be known beforehand via some suitable measurements. In case K is not known beforehand, then K should be estimated or correlated as a function of wind velocity, i.e., $K = f(v_a)$. This estimation can be performed during the experiment with the data obtained by sensors (e.g. anemometers, gas sensors).*

The diffusion-advection model provided [41], [42] has been recalled here to simulate the dynamic plume under time varying disturbances. Initial conditions have been chosen to be far from the equilibrium point. We shall consider a time varying disturbance $\varsigma_i = 0.3\sin(\pi^2 t^2)$ for matched case and $\varsigma_i = 20\sin(\pi^2 t^2)$ for mismatched case, accuracy parameter $\theta = 0.001$ and maximum mean airflow velocity $\bar{v}_{a_{max}} = 1$ m/s. Other key design parameters are provided in table I.

TABLE I: Values of the design parameters used in simulation

k_1	ω_{max}	α_1	α_2	λ_1	λ_2	μ	m	w
0.5	2 rad/s	0.25	0.25	1.774	2.85	5	10^{-3}	2

A steady concentration profile for a very large span of time $(t \to \infty)$ can be written as

$$C(\vec{\boldsymbol{r}}, \infty) = \frac{q_0}{2\pi K d_i} \exp\Big\{ -\frac{v_a}{2K}(d_i - \vec{\boldsymbol{r}} + \vec{\boldsymbol{r}}_0)\Big\}. \tag{44}$$

In (44), $\vec{\boldsymbol{r}}_0 = x_s(t)$ represents the coordinates of the odour source, $d_i = \|x_i - x_s\|$, q_0 is the filament release rate and K is the turbulent diffusion coefficient that is independent of the diffusing material. K is taken to be 0.02 m^2/sec and $q_0 = 2$ mg/sec of diffusing substance. We shall present the results for both the cases of localisation in $\mathbb{R}^1$ and $\mathbb{R}^2$ to demonstrate the efficiency of the designed control scheme.

For the case of $\mathbb{R}^1$, the odour source is randomly placed between 10 m and 11 m, as shown in figure 3. Agents and their respective trajectories are represented by five different colours. The odour source is represented by a grey circle, and the filaments released from the odour source are represented as black dots. Agents start from various initial conditions that are far from the origin. Reference for agents is taken from left hand vertical axis and that for the source is taken from right hand vertical axis. Agents start moving from left hand side to progress towards the source via instantaneous plume sensing (by sensing odour molecules, or filaments). As soon as the leader agent senses the odour molecules, the information of predicted next state is exchanged among other agents. This local information is then used to make a consensus while localisation. It is evident that agents come to consensus in finite time to locate the odour source. In spite of time varying disturbance, the plume tracking is accurate and the localisation is successful. In figure 4, agents locate the odour source in parallel formation. During parallel formation, a fixed distance is maintained between two consecutive agents. In both the cases, filaments or odour molecules (source information) are released from the odour source and are detected by the sensors equipped with the agents. Although the filaments disperse throughout the domain, only the source information relevant to the agents has been shown in the figure. The agents start from left and progress towards the source to the right. The tracking controller attempts to minimise the error between the predicted next state and the actual next state. The tracking error lies in the close vicinity of zero as expected, implying that the tracking error has almost been nullified. Norm of tracking errors in $\mathbb{R}^1$ has been depicted in figure 5 to depict near nullification of error. Sliding manifolds, which has been designed to be novel in this study, also come to consensus in very short span of time, as evident from figure 5. It is, then, quite clear that the convergence of state trajectories to the sliding manifold is very fast, and is highly desired to ensure a high degree of robustness and autonomy. Such manifolds can also be utilised to attain a desired convergence speed by simple tuning of design parameters. Use of a novel inverse sine hyperbolic reaching law results in a smooth control signals

for all the agents. The use of smooth sliding mode controller ensures safe operation in mechatronic devices. Figure 6 depicts the control signals of all the agents when localisation is carried in $\mathbb{R}^1$. It is clear that the signal is chattering free, smooth and accurate.

Having discussed the case of $\mathbb{R}^1$, we shall now discuss the odour source localisation in $\mathbb{R}^2$. To avoid confusion between state variable x and axis labelled as x in the usual sense, we have adopted to refer abscissa as first axis and ordinate as second axis throughout this discussion. Agents are driven into consensus to locate the odour source in $\mathbb{R}^2$ in the domain described by the axis limits. Within the domain of localisation, a total of 25 trials were done with various initial conditions chosen far from the origin. Figure 7 shows the average time spent in four cases– localisation via consensus under matched perturbations (Case 1), localisation via formation under matched perturbations (Case 2), localisation via consensus under mismatched perturbations (Case 3), and localisation via formation under mismatched perturbations (Case 4). Similar to the results in [43], the success rate of this technique is also 100% except for the fact that time spent in localisation is lesser via this technique owing to faster convergence of state trajectories to the sliding manifold. The four cases have been illustrated here in a tabular format for ease of reference. A check (cross) mark in a particular column indicates that the particular strategy has been used (not used) in localisation.

TABLE II: Four cases of localisation considered in this study

Technique	Consensus	Formation	Matched perturbations	Mismatched perturbations
Case 1	✓	×	✓	×
Case 2	×	✓	✓	×
Case 3	✓	×	×	✓
Case 4	×	✓	×	✓

We shall also present two cases under which localisation has been tasked– under consensus and under parallel formation. Note that agents may be subjected to any geometrical pattern, or formation that deems suitable for the task at hand. Figure 8 depicts wind turbulence in the domain during localisation via consensus. Snapshots in four segments of time have been taken, as described in figure 8. The first snapshot is taken randomly between $0 < t < 2.5$ sec and the velocity plot depicting turbulence at that time has been presented. Wind turbulence for the case of localisation via formation has been illustrated by velocity plots in figure 9 similar to that in figure 8. In figure 10, norms of tracking error candidates along first and second axis have been depicted. Similar to the error profile in figure 5, the tracking is accurate and the agents are able to complete the localisation task in finite time. For a random trial, figure 11 shows localisation in a turbulent environment under the effect of both mismatched and matched disturbances. Under mismatched disturbances and turbulence, localisation takes slightly more time as compared with its matched disturbance counterpart. Two best case scenarios have been also presented in figures 12 and 13 to illustrate the efficacy of the proposed scheme. Figure 12 shows the localisation under consensus in $\mathbb{R}^2$. The domain for this task has been set to be a grid of 50×50 along both the axes. Abscissa ranges from -20 to 30, and so does the ordinate. Start position of agents are denoted by a $\times$ in five different colours. Filaments or the odour molecules are released from the odour source and the molecules disperse in the domain. Figure 13 shows agents making parallel formation in $\mathbb{R}^2$ to locate the source (domain of localisation is defined via axis limits, which happens to be a grid of 80×80). In the formation case, abscissa and ordinate range from -20 to 60. The explanation is similar to that for the case of localisation via consensus. The performance metrics of the localisation in terms of average time spent to locate the source of odour have been provided in table III.

TABLE III: Performance metrics in context of localisation

Technique	Average Success rate	Median localisation Time	Control Implementation
Case 1 (this study)	100%	16 sec	Time-triggered
Case 2 (this study)	100%	20 sec	Time-triggered
Case 3 (this study)	100%	18 sec	Time-triggered
Case 4 (this study)	100%	22 sec	Time-triggered
PSO [44]	21.5%	986.25 sec	Time-triggered
FTMCS [43]	100%	137.5 sec	Time-triggered

VI. Conclusion

In this paper, odour source localisation via multi-agent systems has been addressed. The localising task is based on a cooperative strategy where agents interact locally among themselves to locate the source of odour in finite time. A hierarchical control scheme has been developed to predict the probable location of odour source using information of wind and concentration. This control scheme based on PSO and SMC is robust and insensitive to matched disturbances. Numerical simulations demonstrate the effectuality of the proposed scheme for both cases– when agents localise the odour source via consensus, and parallel formation. The localisation takes very less time compared to other strategies and the success rate is 100%. In future, we shall address the communication issues associated with the problem.

References

[1] G. S. Settles, "Sniffers: Fluid-dynamic sampling for olfactory trace detection in nature and homeland security–the 2004 freeman scholar lecture," *Journal of Fluids Engineering*, vol. 127, no. 2, pp. 189–218, Feb 2005. [Online]. Available: http://dx.doi.org/10.1115/1.1891146

[2] D. W. Gage, "Many-robot mcm search systems," in *Proceedings of Autonomous Vehicles in Mine Countermeasures Symposium*, 1995, pp. 9–55.

[3] H. Ishida, T. Nakamoto, T. Moriizumi, T. Kikas, and J. Janata, "Plume-tracking robots: A new application of chemical sensors," *The Biological Bulletin*, vol. 200, no. 2, pp. 222–226, 2001, pMID: 11341588. [Online]. Available: https://doi.org/10.2307/1543320

[4] V. Formisano, S. Atreya, T. Encrenaz, N. Ignatiev, and M. Giuranna, "Detection of methane in the atmosphere of mars," *Science*, vol. 306, no. 5702, pp. 1758–1761, 2004. [Online]. Available: http://science.sciencemag.org/content/306/5702/1758

[5] V. A. Krasnopolsky, J. P. Maillard, and T. C. Owen, "Detection of methane in the martian atmosphere: evidence for life?" *Icarus*, vol. 172, no. 2, pp. 537 – 547, 2004. [Online]. Available: http://www.sciencedirect.com/science/article/pii/S0019103504002222

[6] J. A. Farrell, S. Pang, and W. Li, "Plume mapping via hidden markov methods," *IEEE Transactions on Systems, Man, and Cybernetics, Part B (Cybernetics)*, vol. 33, no. 6, pp. 850–863, Dec 2003.

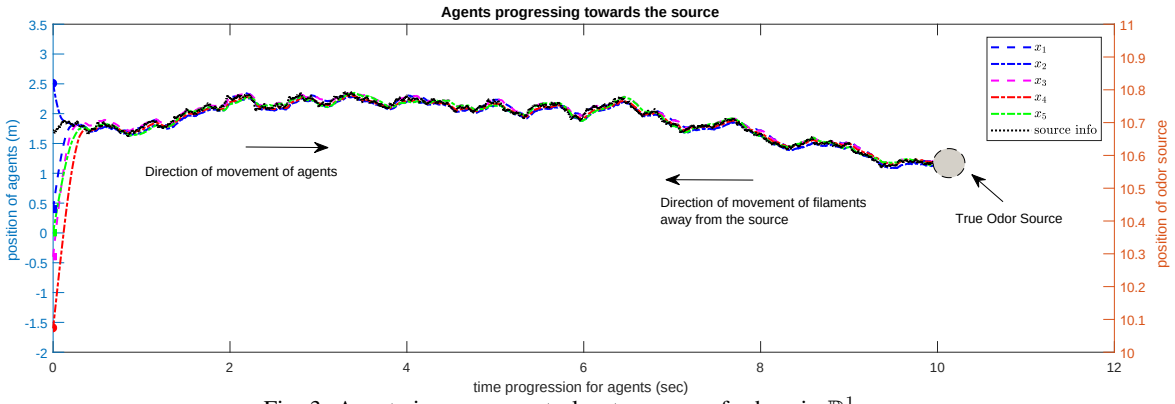

Fig. 3: Agents in consensus to locate source of odour in $\mathbb{R}^1$

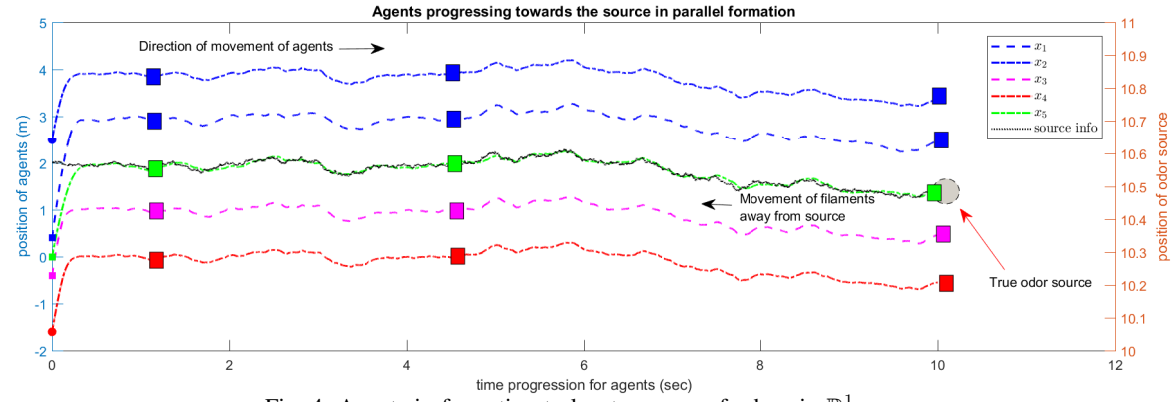

Fig. 4: Agents in formation to locate source of odour in $\mathbb{R}^1$

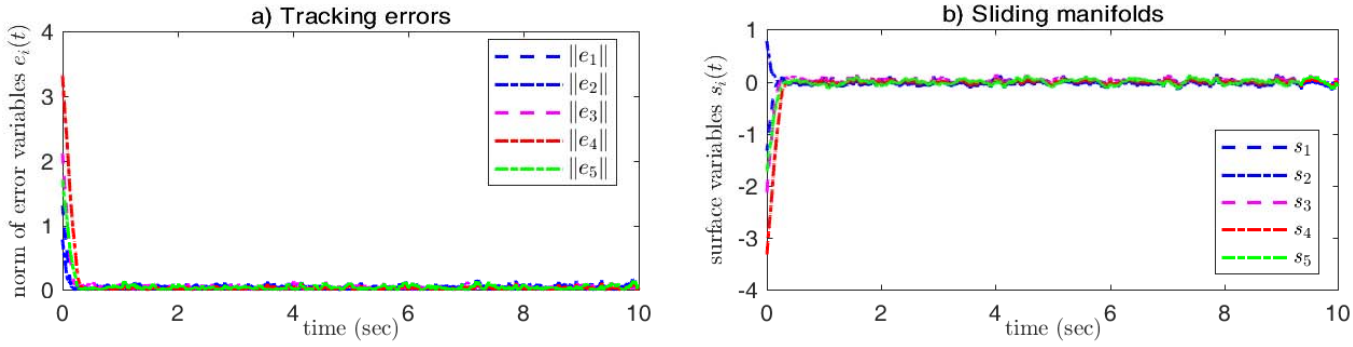

Fig. 5: a) localisation tracking errors in $\mathbb{R}^1$ b) sliding manifolds during consensus

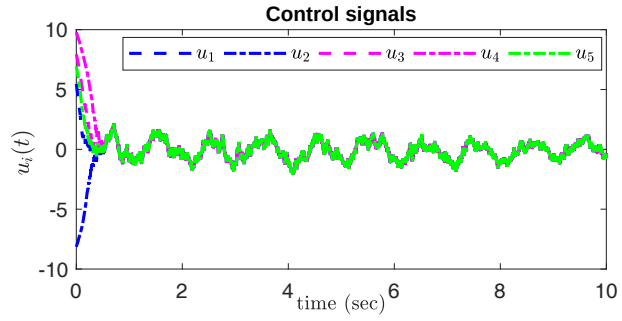

Fig. 6: Smooth control signals of all the agents during consensus

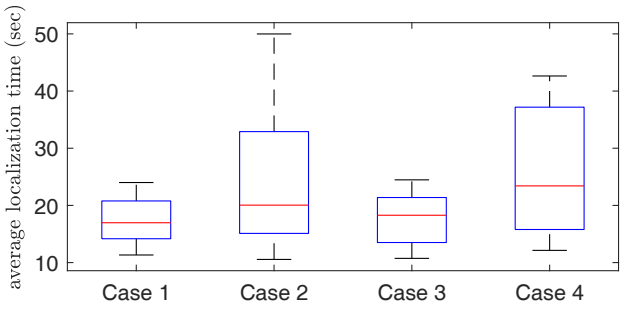

Fig. 7: Average localisation time for 25 trials

[7] M. Vergassola, E. Villermaux, and B. Shraiman, ""Infotaxis" as a strategy for searching without gradients," *Nature*, vol. 445, no. 7126,

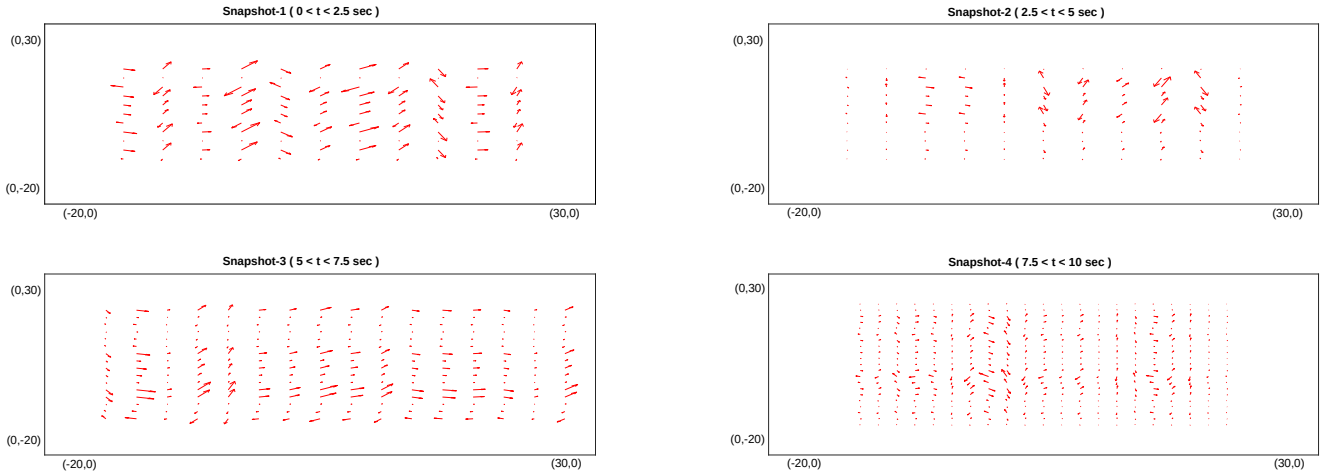

Fig. 8: Wind turbulence in the domain during localisation via consensus

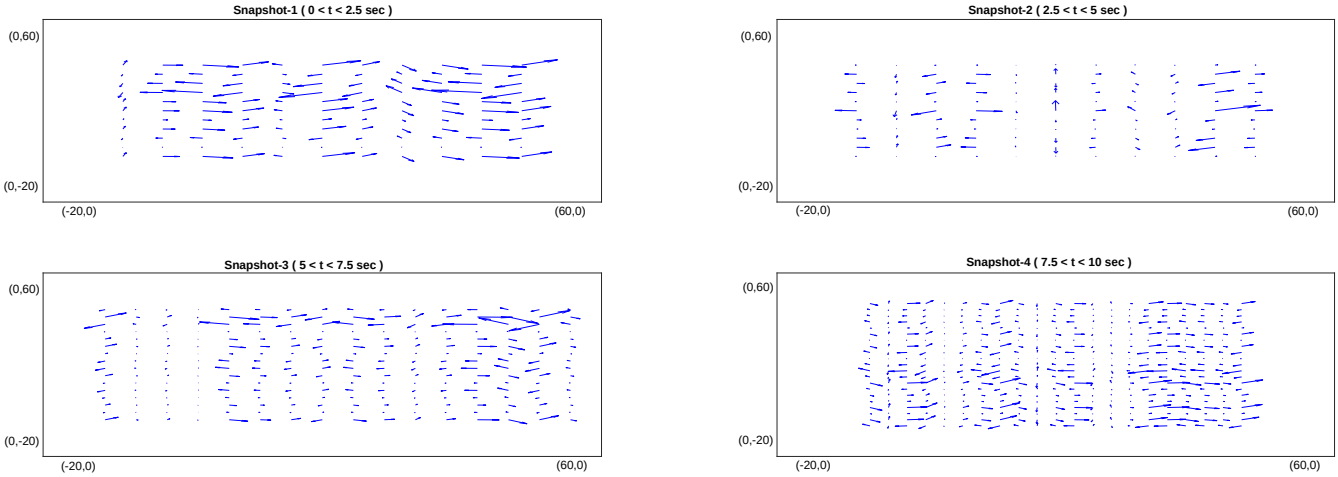

Fig. 9: Wind turbulence in the domain during localisation via formation

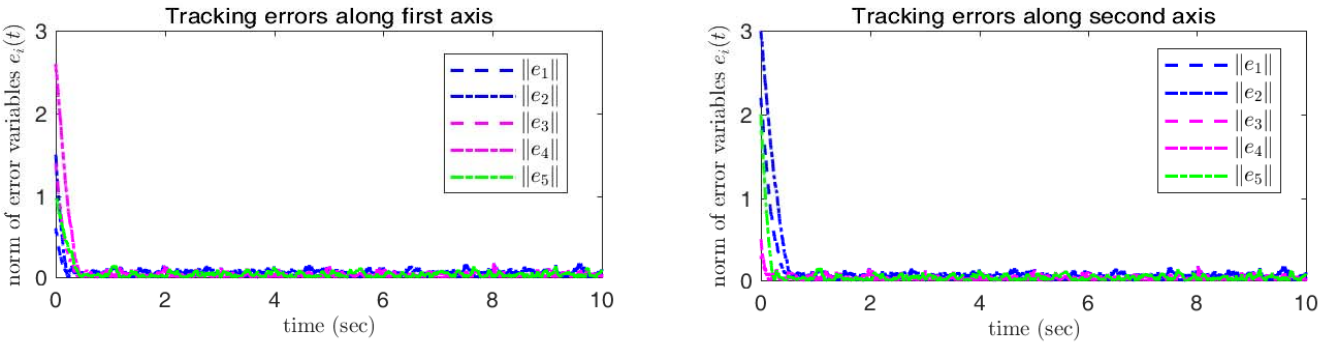

Fig. 10: localisation tracking errors along both the axes in $\mathbb{R}^2$

pp. 406–409, 2007. [Online]. Available: https://hal.archives-ouvertes.fr/hal-00326807

[8] A. Sinha, R. Kaur, R. Kumar, and A. P. Bhondekar, "Cooperative control of multi-agent systems to locate source of an odor," *ArXiv e-prints*, Nov. 2017.

[9] X. Cui, C. T. Hardin, R. K. Ragade, and A. S. Elmaghraby, "A swarm approach for emission sources localization," in *16th IEEE International Conference on Tools with Artificial Intelligence*, Nov 2004, pp. 424–430.

[10] C. Lytridis, G. S. Virk, Y. Rebour, and E. E. Kadar, "Odor-based navigational strategies for mobile agents," *Adapt. Behav.*, vol. 9, no. 3-4, pp. 171–187, Apr. 2001. [Online]. Available: http://dx.doi.org/10.1177/10597123010093004

[11] R. Rozas, J. Morales, and D. Vega, "Artificial smell detection for robotic navigation," in *Advanced Robotics, 1991. 'Robots in Unstructured Environments', 91 ICAR., Fifth International Conference on*, June 1991, pp. 1730–1733 vol.2.

[12] V. Genovese, P. Dario, R. Magni, and L. Odetti, "Self organizing behavior and swarm intelligence in a pack of mobile miniature robots

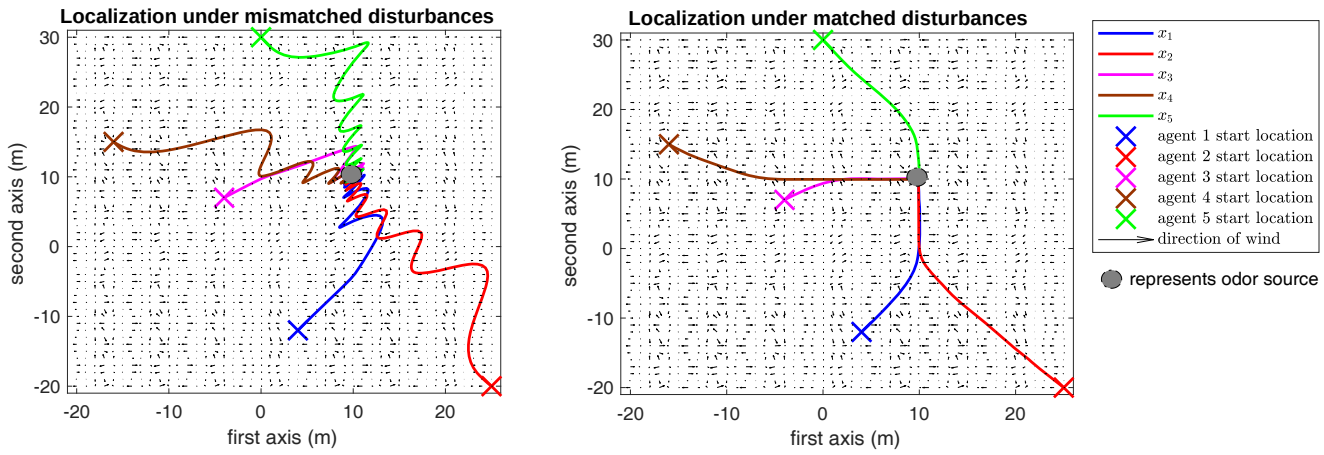

Fig. 11: localisation by MAS under the effect of mismatched and matched disturbances

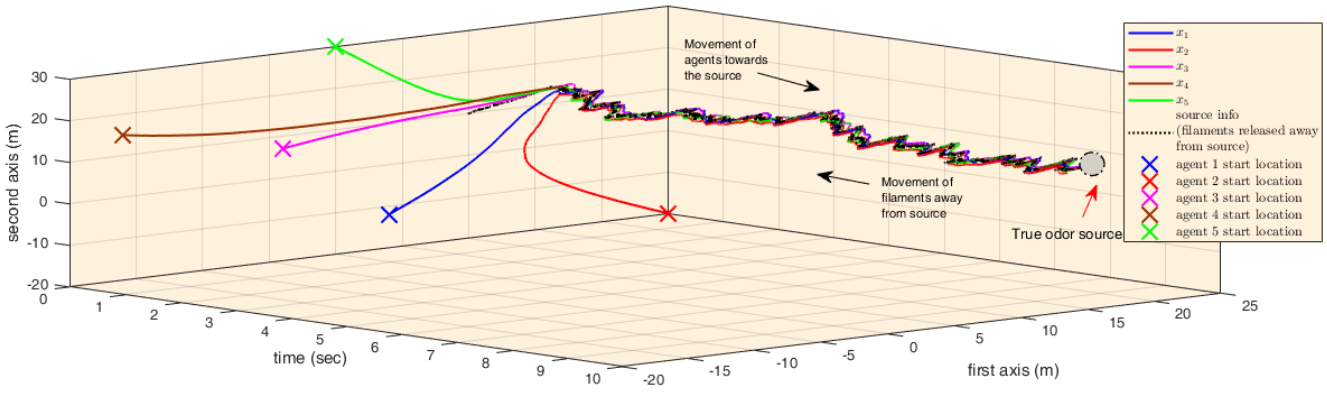

Fig. 12: Agents in consensus to locate source of odour in $\mathbb{R}^2$

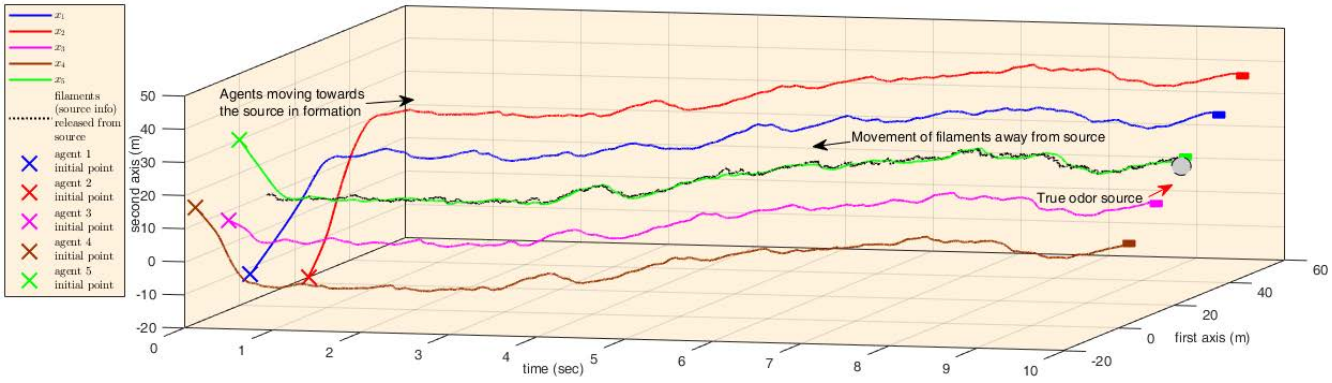

Fig. 13: Agents in formation to locate source of odour in $\mathbb{R}^2$

in search of pollutants," in *Proceedings of the IEEE/RSJ International Conference on Intelligent Robots and Systems*, vol. 3, Jul 1992, pp. 1575–1582.

[13] L. Buscemi, M. Prati, and G. Sandini, "Cellular robotics: Behaviour in polluted environments," in *Proceedings of the 2nd International Symposium on Distributed Autonomous Robotic Systems*, 1994.

[14] M. H. E. Larcombe, *Robotics in nuclear engineering: Computer assisted teleoperation in hazardous environments with particular reference to radiation fields*. United States: Graham and Trotman, Inc, 1984.

[15] R. Russell, *Chemical source location and the RoboMole project*. Australian Robotics and Automation Association, 2003, pp. 1 – 6.

[16] R. A. Russell, "Locating underground chemical sources by tracking chemical gradients in 3 dimensions," in *2004 IEEE/RSJ International Conference on Intelligent Robots and Systems (IROS) (IEEE Cat. No.04CH37566)*, vol. 1, Sept 2004, pp. 325–330 vol.1.

[17] Russell, R. Andrew, "Robotic location of underground chemical sources," *Robotica*, vol. 22, no. 1, pp. 109–115, 2004.

[18] D. Martinez, L. Perrinet, and D. Walther, "Cooperation between vision and olfaction in a koala robot," in *Report on the 2002 Workshop on Neuromorphic Engineering*, 2002, pp. 51–53.

[19] A. Loutfi, S. Coradeschi, L. Karlsson, and M. Broxvall, "Putting olfaction into action: using an electronic nose on a multi-sensing mobile robot," in *2004 IEEE/RSJ International Conference on Intelligent Robots and Systems (IROS) (IEEE Cat. No.04CH37566)*, vol. 1, Sept 2004, pp.

337–342 vol.1.
[20] H. Ishida, K. Yoshikawa, and T. Moriizumi, "Three-dimensional gas-plume tracking using gas sensors and ultrasonic anemometer," in *Proceedings of IEEE Sensors, 2004.*, Oct 2004, pp. 1175–1178 vol.3.
[21] R. Russell, A. Bab-Hadiashar, R. L. Shepherd, and G. G. Wallace, "A comparison of reactive robot chemotaxis algorithms," *Robotics and Autonomous Systems*, vol. 45, no. 2, pp. 83 – 97, 2003. [Online]. Available: http://www.sciencedirect.com/science/article/pii/S0921889003001209
[22] S. Pang and J. A. Farrell, "Chemical plume source localization," *IEEE Transactions on Systems, Man, and Cybernetics, Part B (Cybernetics)*, vol. 36, no. 5, pp. 1068–1080, Oct 2006.
[23] D. Zarzhitsky, "Physics-based approach to chemical source localization using mobile robotic swarms," Ph.D. dissertation, University of Wyoming, Laramie, WY, USA, 2008, aAI3338814.
[24] V. Braitenberg, *Vehicles: Experiments in Synthetic Psychology*. Boston, MA, USA: MIT Press, 1984.
[25] H. Ishida, K. Suetsugu, T. Nakamoto, and T. Moriizumi, "Study of autonomous mobile sensing system for localization of odor source using gas sensors and anemometric sensors," *Sensors and Actuators A: Physical*, vol. 45, no. 2, pp. 153 – 157, 1994. [Online]. Available: http://www.sciencedirect.com/science/article/pii/0924424794008299
[26] L. Marques and A. T. D. Almeida, "Electronic nose-based odour source localization," in *6th International Workshop on Advanced Motion Control. Proceedings (Cat. No.00TH8494)*, April 2000, pp. 36–40.
[27] L. Marques, U. Nunes, and A. T. de Almeida, "Olfaction-based mobile robot navigation," *Thin Solid Films*, vol. 418, no. 1, pp. 51 – 58, 2002, proceedings from the International School on Gas Sensors in conjunction with the 3rd European School of the NOSE Network. [Online]. Available: http://www.sciencedirect.com/science/article/pii/S004060900200593X
[28] C. W. Reynolds, "Flocks, herds and schools: A distributed behavioral model," *SIGGRAPH Comput. Graph.*, vol. 21, no. 4, pp. 25–34, Aug. 1987. [Online]. Available: http://doi.acm.org/10.1145/37402.37406
[29] W. Ren and R. W. Beard, "Consensus seeking in multiagent systems under dynamically changing interaction topologies," *IEEE Transactions on Automatic Control*, vol. 50, no. 5, pp. 655–661, May 2005.
[30] R. Olfati-Saber, J. A. Fax, and R. M. Murray, "Consensus and cooperation in networked multi-agent systems," *Proceedings of the IEEE*, vol. 95, no. 1, pp. 215–233, Jan 2007.
[31] W. Yu, G. Chen, W. Ren, J. Kurths, and W. X. Zheng, "Distributed higher order consensus protocols in multiagent dynamical systems," *IEEE Transactions on Circuits and Systems I: Regular Papers*, vol. 58, no. 8, pp. 1924–1932, Aug 2011.
[32] Hayes, Adam T. and Martinoli, Alcherio and Goodman, Rodney M., "Swarm robotic odor localization: Off-line optimization and validation with real robots," *Robotica*, vol. 21, no. 4, pp. 427–441, Aug. 2003. [Online]. Available: http://dx.doi.org/10.1017/S0263574703004946
[33] J. Kennedy and R. Eberhart, "Particle swarm optimization," in *Neural Networks, 1995. Proceedings., IEEE International Conference on*, vol. 4, Nov 1995, pp. 1942–1948 vol.4.
[34] W. Jatmiko, K. Sekiyama, and T. Fukuda, "A pso-based mobile robot for odor source localization in dynamic advection-diffusion with obstacles environment: theory, simulation and measurement," *IEEE Computational Intelligence Magazine*, vol. 2, no. 2, pp. 37–51, May 2007.
[35] Q. Lu, S. r. Liu, and X. n. Qiu, "A distributed architecture with two layers for odor source localization in multi-robot systems," in *IEEE Congress on Evolutionary Computation*, July 2010, pp. 1–7.
[36] Q. Lu and Q. L. Han, "Decision-making in a multi-robot system for odor source localization," in *IECON 2011 - 37th Annual Conference of the IEEE Industrial Electronics Society*, Nov 2011, pp. 74–79.
[37] Q. Lu, S. Liu, X. Xie, and J. Wang, "Decision making and finite-time motion control for a group of robots," *IEEE Transactions on Cybernetics*, vol. 43, no. 2, pp. 738–750, April 2013.
[38] J. A. Farrell, J. Murlis, X. Long, W. Li, and R. T. Cardé, "Filament-based atmospheric dispersion model to achieve short time-scale structure of odor plumes," *Environmental Fluid Mechanics*, vol. 2, no. 1, pp. 143–169, Jun 2002. [Online]. Available: https://doi.org/10.1023/A:1016283702837
[39] Fan R. K. Chung, *Spectral Graph Theory*, ser. CBMS Regional Conference Series in Mathematics. AMS and CBMS, 1997, vol. 92. [Online]. Available: http://bookstore.ams.org/cbms-92
[40] K. David Young, Vadim I. Utkin and Umit Ozguner, "A control engineer's guide to sliding mode control," *IEEE transactions on Control Systems Technology*, vol. 7, no. 3, pp. 328–342, May 1999.
[41] M. L. Cao, Q. H. Meng, Y. X. Wu, M. Zeng, and W. Li, "Consensus based distributed concentration-weighted summation algorithm for gas-leakage source localization using a wireless sensor network," in *Proceedings of the 32nd Chinese Control Conference*, July 2013, pp. 7398–7403.
[42] J. Matthes, L. Groll, and H. B. Keller, "Source localization by spatially distributed electronic noses for advection and diffusion," *IEEE Transactions on Signal Processing*, vol. 53, no. 5, pp. 1711–1719, May 2005.
[43] Q. Lu, Q. L. Han, X. Xie, and S. Liu, "A finite-time motion control strategy for odor source localization," *IEEE Transactions on Industrial Electronics*, vol. 61, no. 10, pp. 5419–5430, Oct 2014.
[44] L. Marques, U. Nunes, and A. T. de Almeida, "Particle swarm-based olfactory guided search," *Autonomous Robots*, vol. 20, no. 3, pp. 277–287, Jun 2006. [Online]. Available: https://doi.org/10.1007/s10514-006-7567-0